Spectroscopic study of titanium dioxide thin films prepared by pulsed laser deposition

Rahaf Nasri, Kamal Kayed[*] and Hammoud Al-ourabi

Department of physics - Faculty of Science - University of Damascus - Syria.

*E-mail: khmk2000@gmail.com

Abstract

This paper aims to investigate the target type effect on some spectroscopic features of titanium dioxide thin films prepared by laser ablation method. The results of the structural study showed that the sample deposited by using a metallic Ti target contains a large proportion of developed rutile phase, but if the target is pressured annealed disc of TiO_2 consists mainly of anatase phase. We also found that the use of metal targets leads to higher optical transparency and higher energy band gap.

Keywords: Titanium dioxide; Thin Film; laser ablation; annealing.

1. Introduction

Titanium dioxide is one of the extensively studied transition-metal oxides [1] due to its photo(electro)chemical stability and photo activity as well as its non-toxicity and low cost[2], It has wide applications such as solar cells, gas sensors, air purification[3], water remediation [4], anodes for lithium ion batteries, self-cleaning glasses[5], cosmetics[6] and antireflection coatings[7].

TiO_2 can exist in three basic crystalline phases: anatase (tetragonal), rutile (tetragonal), brookite (orthorhombic), and an amorphous phase [8]. TiO_2 thin films are commonly used because of their desirable properties, such as chemical stability, good adhesion, and high stability against mechanical abrasion and high temperatures [9]

Many deposition methods have been used to prepare titanium films. Physical methods such as DC or RF magnetron sputtering [10], thermal evaporation [8], electron beam evaporation [11], pulsed laser deposition (PLD)[12], and chemical methods such as spin coating of sol gel precursors [6], chemical vapor deposition (CVD)[13].

In this paper we have used pulsed laser deposition (PLD) as a preparation technique because of its advantages. In this method the ablation of the target preserves its stoichiometry in the thin film [14]. It is also enables us to have many choices of target materials, ambient gas and pressures. This gives us the ability to get different types of films that have various structures [15].

2. Materials and Methods

Two samples (**a** and **b**) of Titanium dioxide thin films were deposited on silicon and glass substrates by pulsed-laser deposition (PLD) using Q-switched Nd:YAG pulsed laser from a high-purity targets mounted in a vacuum chamber with background pressure of 1×10^{-4} Pa. The samples were deposited using pure oxygen molecular gas at pressure of 10 Pa, and deposition time = 10 minutes. Sample (**a**) was deposited by using a metallic Ti target while sample (**b**) was deposited by using a pressed annealed disc of TiO_2. The distance between the substrate and the target was 2 cm. The laser beam was focused on the target at an incidence angle of 45°. The deposited films were annealed in air at 400 C°.

Infrared (IR) absorption spectra of CN_x thin films were carried out using a Bruker Vertex 7 Fourier transform IR spectrophotometer with resolutions of 4 cm^{-1}. We were taking as reference a silicon substrate. The thickness of the films are determined from the cross-section image analyzed by scanning electron microscope (SEM) using a JEOL-type JSM 6400F. The thickness of the sample (a) and sample (b) were measured to be about 28.1 nm

and 57.9 nm respectively. The surface profile, particle sizes and surface roughness of the were examined using Atomic Force Microscopy (AFM, Nanosurf easyScan2, Switzerland).The optical transmittance measurements of TiO_2 thin films was performed by using a UV-Vis spectrophotometer (CARY 5000) with integrating sphere (DRA- 2500) was used to measure the total surface reflectance in the wavelength range from 300 to 800 nm.

3. Results and Discussion

Figure 1 shows the FT-IR transmittance spectra of the two samples. In the case of sample (a), we observed a peak around 445 cm^{-1}, which is the typical characteristic of Ti-O-Ti transverse mode of rutile [17]. The peak at 555 cm^{-1} indicates the presence of titanium metal. In the case of sample (b), we observed two peaks at 431 and 582 cm^{-1} which are assigned to stretching mode of anatase [18]. A set of peaks appeared in both spectra: the peaks observed at 1075 cm^{-1} is assigned to C-O stretching mode, where the peaks observed at 667 cm^{-1} and 1246 cm^{-1} are assigned to C = O stretching mode. The peak appear around 475 cm^{-1} could be originated from the presence of Ti─O─Ti bonds [17,18].
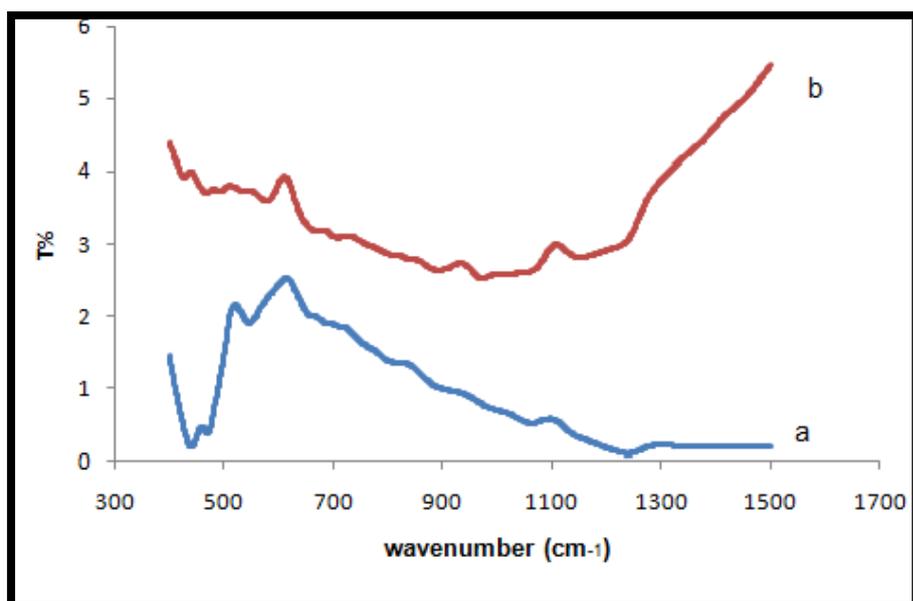

Fig. 1: FT-IR spectra for the two samples.

The elemental compositions analyzed with X-ray energy-dispersive spectroscope are shown in table 1. We note that there is a similarity in the components of the films but the percentage of oxygen is slightly lower in the sample (b). Carbon is the result of adsorption on the surface of the films.

Table 1: The elemental compositions analyzed with X-ray energy-dispersive spectroscope

Sample a			Sample b		
Element	Weight %	Atomic %	Element	Weight %	Atomic %
C K	5.31	8.37	C K	7.48	11.76
O K	68.9	81.45	O K	65.94	77.77
Ti K	25.79	10.18	Ti K	26.58	10.47

The transmittance spectra of the TiO_2 prepared films in the wavelengths range of 300–800 nm are shown in Fig. 2. We notice that sample (**a**) has a higher optical transparency compared with the case of sample (**b**). The transmittance difference is the result of several factors; the most important is different thickness, density and crystalline structure.
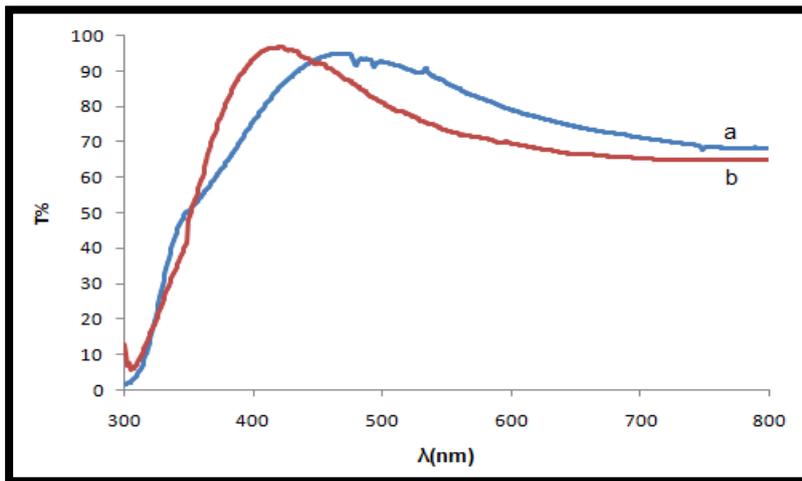

Fig. 2: the optical transmissions for the prepared samples.

On the other hand, it can be seen that the transmittance spectra show a resonant increase in transmittance at wavelength of 458 nm for sample **(a)** and 410 nm for sample **(b),** which can be due to the localized surface plasmon, and scattering of photons, which is caused by photon-electron interaction decreases the transmittance at longer wavelengths [10]. The peak position shift from 410 nm (sample b) to 458 nm (sample a) indicate that sample (a) has a larger plasmon particle size compared with sample (b). On the other hand, we can notice in fig. 2 that the plasmon absorption band of the sample (a) is larger than that of sample (a) which means that sample (b) has higher density of plasmon particles. These results are consistent with the results of EDX measurements (table 1) where we note that sample (b) has the least oxygen content and the higher titanium metal content. These conditions allow for a higher proportion of free titanium atoms that form plasmon. Free metal atoms arise as a result of disintegration of the TIO_2 oxide when exposed to the laser beam.

Regardless of the effects of plasmon formation, there is no significant difference in the optical transmissions between the two samples. Taking into account the thickness of the two samples, we conclude that to obtain equal values of the optical transmissions, sample (a) should be of high density compared to the sample (b).

The curves in figure 3 are used to calculate the absorption coefficient and the optical energy gap. The optical gap was calculated for all samples using the relation [19]:

$$\alpha h\upsilon = A(h\upsilon - E_g)^{1/2} \qquad (2)$$

Where Eg is the optical band gap and **A** is a constant. The value of E_g can be found by plotting the variation of $(\alpha h\upsilon)^2$ against $h\upsilon$, where the extrapolation of the linear region of the curve with X-axis gives the value of the optical band gap of a thin film. Fig. 3 shows the method of calculating of the energy band gap of samples.
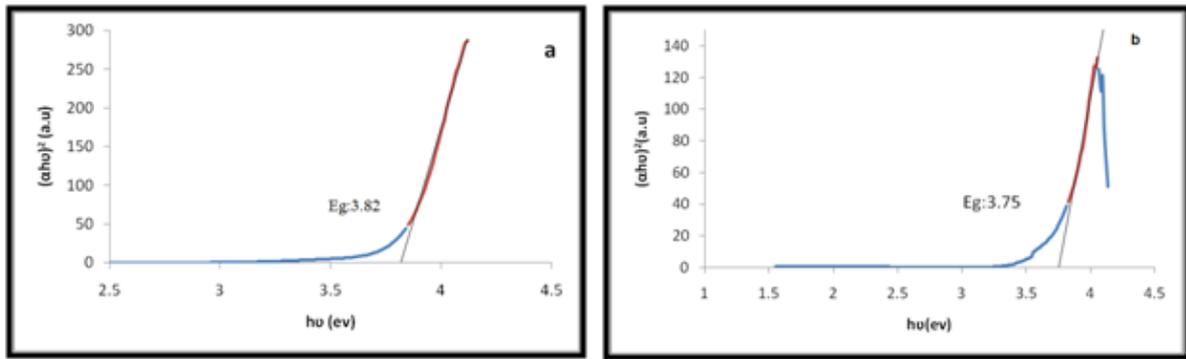
Fig. 3: variation of $(\alpha h\upsilon)^2$ against hυ for samples.

The band gap of the sample (**a**) was 3.82 eV, and the band gap of the sample (**b**) was 3.75 eV. The decrease in the band gab of sample (b) compared to the sample (a) is consistent with EDX measurements (table 1) where we found that sample (b) has a high concentration of plasmon compared to sample (a). Another possible reason is the crystalline structure changes and the formation of the anatase phase.

The three-dimensional AFM images of prepared films are presented by AFM images were as shown in Fig 4. The microstructures of the thin films changed depending on the target type. We notice that Films have a continuous nanoscale structure with no well-defined grain boundaries. On other hand, sample (**b**) contains more grain and semi-larger diameters compared to the grain in sample (**a**) and the roughness of the sample (a) is 0.60 nm, while the roughness of the sample (b) is 0.85.
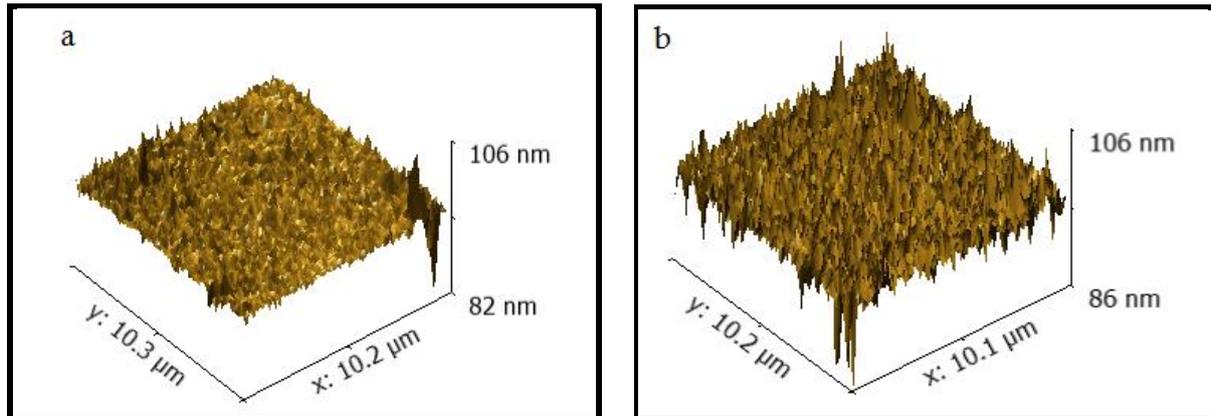
Fig. 4: AFM images for the two samples.

4. Conclusion

TiO$_2$ thin films were successfully synthesized on silicon and glass substrates using PLD techniques with subsequent annealing in air. The structural and optical properties of TiO$_2$ thin films were investigated using FTIR and UV-Vis spectroscopes. Results showed that the crystal structure of the film is largely related to the type of target used during the preparation process. In the case of using Ti target we obtain a lower concentration of surface plasmon, put in the case of using TiO$_2$ target, we obtain a higher surface plasmon concentration with smaller plasmon particle size. Also, we found that the use of metal targets leads to higher optical transparency and lower energy band gap.

Acknowledgments

References

[1] B. Karunagaran, K. Kim, D. Mangalaraj, J. Yi, Solar energy materials and solar cells. 88.2 (2005) 199-208.

[2] Z. Wu, Y. Xue, Z. Zou, X.Wang, F. Gao, Journal of colloid and interface science. 490(2017) 420-429.

[3] E. Boonen, A. Beeldens, Coatings. 4.3(2014) 553-573

[4] G. Balasubramanian, D.D. Dionysiou, M. T. Suidan, I. Baudin, J.M. Laıné, Applied Catalysis B:Environmental. 47.2 (2004) 73-84.

[5] W. Promnopas, S.Promnopas, T. Phonkhokkong, T. Thongtem, D. Boonyawan, L. Yu, S. Thongtem, Surface and Coatings Technology. 306 (2016) 69-74.

[6] V.Vetrivel, K. Rajendran, V.Kalaiselvi, Int. J. ChemTech Res. 7 (2015) 1090-1097.

[7] N. M. Said, M. Z. Sahdan, I. Senain, A. S. Bakri, S. A. Abdullah, F. Mokhter, H. Saim, ARPN Journal of Engineering and Applied Sciences.11 (2006) 4924-4928.

[8] L.Bedikyan, S. Zakhariev, M. Zakharieva, Journal of Chemical Technology and Metallurgy. 48.6 (2013), 555-558.

[9] A. Dakka, J. Lafait, M. Abd-Lefdil, C. Sella, MJ Condensed matter. 2.1 (1999), 153-156.

[10] M. A. El-Raheem, A. M. Al-Baradi, Journal of Physical Sciences. 8.31 (2013)1570-1580.

[11] Z. J. Xu, F. Zhang, R. J. Zhang, X. Yu, D. X. Zhang, Z. Y. Wang, L. Y. Chen, Applied Physics A. 113.3 (2013) 557-562.

[12]] Y. Xu, M. Shen, Journal of materials processing technology. 202.1-3 (2008) 301-306.

[13] K. H. Ahn, Y. B. Park, D. W. Park, Surface and Coatings Technology. 171.1-3 (2003)198-204.

[14] S.S. A l-Obaidi, Y. Yousif, Ibn AL-Haitham Journal For Pure and Applied Science. 26.3 (2017) 143-152.

[15] T. Nakamura, E. Matsubara, N. Sato, A. Muramatsu, H. Takahashi, Materials transactions. 45.7 (2004) 2068-2072.

[16] H. Yang, S. Zhu, N. Pan, Journal of Applied Polymer Science. 92.5 (2004) 3201-3210.

[17] T. Ivanova, A. Harizanova, T. Koutzarova, B. Vertruyen, Journal of Physics: Conference Series. IOP Publishing. 764.1 (2016) 012019.

[18] N. R. Khalid, E. Ahmed, A. Rasheed, M. Ahmad, M. Ramzan, A. Shakoor, N. A. Niaz, J. Ovonic Res. 11(2015) 107-112.

[19] N. Mott, E. Davis, Electronic properties in non-crystalline materials, 1st edition, Oxford University (1971).